analytical chemistry

Article

pubs.acs.org/ac

Continuous Flow ^{1}H and ^{13}C NMR Spectroscopy in Microfluidic Stripline NMR Chips

Anna Jo Oosthoek-de Vries,[†] Jacob Bart,[†,‡,§] Roald M. Tiggelaar,[‡] Johannes W. G. Janssen,[†] P. Jan M. van Bentum,[†] Han J. G. E. Gardeniers,[‡] and Arno P. M. Kentgens*[,†]

[†]Institute of Molecules and Materials, Radboud University, 6525 HP Nijmegen, The Netherlands

[‡]Mesoscale Chemical Systems, MESA+ Institute of Nanotechnology, University of Twente, 7522 NB Enschede, The Netherlands

Supporting Information

ABSTRACT: Microfluidic stripline NMR technology not only allows for NMR experiments to be performed on small sample volumes in the submicroliter range, but also experiments can easily be performed in continuous flow because of the stripline's favorable geometry. In this study we demonstrate the possibility of dual-channel operation of a microfluidic stripline NMR setup showing one- and two-dimensional ^{1}H, ^{13}C and heteronuclear NMR experiments under continuous flow. We performed experiments on ethyl crotonate and menthol, using three different types of NMR chips aiming for straightforward microfluidic connectivity. The detection volumes are approximately 150 and 250 nL, while flow rates ranging from 0.5 μL/min to 15 μL/min have been employed. We show that in continuous flow the pulse delay is determined by the replenishment time of the detector volume, if the sample trajectory in the magnet toward NMR detector is long enough to polarize the spin systems. This can considerably speed up quantitative measurement of samples needing signal averaging. So it can be beneficial to perform continuous flow measurements in this setup for analysis of, e.g., reactive, unstable, or mass-limited compounds.

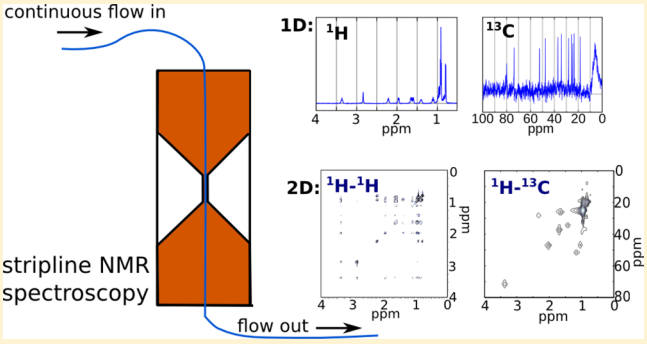

Nuclear magnetic resonance (NMR) spectroscopy is a powerful technique and an important tool for complex molecular structure determination and mixture analysis in biology and chemistry. However, because of the inherent low sensitivity of the technique,[1] relatively large amounts of sample are needed in order to prevent very long signal averaging for obtaining meaningful spectra. Since the signal-to-noise ratio (SNR) of the measurement scales linearly with the number of spins contributing to the signal but scales only with square root of the number of scans, for mass limited samples it can become a problem to achieve sufficient SNR in the time available. Moreover, if the sample volume does not match the coil volume (typically 500 μL for commercial NMR probes), substantial dilution of the sample is needed, and as a consequence the signal of the sample may be obscured by the signal of the solvent. Furthermore, the composition of the sample itself should be constant during the acquisition in order to measure a representative spectrum. In some cases, e.g., for fast reactions and/or long measurements, such as 2D or ^{13}C experiments on unstable compounds, changes in composition of the sample during the total measurement time result in spectra that reflect only an approximation of the average composition of the sample.

A possible solution to these problems is miniaturization, as reducing the diameter of the NMR coil increases the sensitivity per amount of spins.[1,2] Therefore, since the introduction of the first solenoidal microcoils[3,4] and the first planar microcoils,[5] microcoils are an extensively explored topic in NMR research.[6−10] In the past decade, several approaches to microscale NMR include solenoid coils,[11−13] planar coils,[14,15] Helmholtz coils,[16] and striplines/microslots.[17−22]

Microcoils are not only more suited for measuring mass-limited samples, but depending on the design, also in situ measurements in a microfluidic setup are facilitated. In this contribution we investigate the use of stripline NMR microcoils coupled to a standard microfluidic setup for continuous flow NMR. Microfluidic continuous flow NMR can be of importance in chemistry,[23] where in-line analysis can be advantageous especially in applications where samples are unstable or in quantitative high-throughput analysis. Another approach in microfluidic NMR is remote detection NMR,[24−26] where separation of encoding and detection steps results in a higher sensitivity. Some applications of microfluidic NMR focus on in situ monitoring of reaction kinetics (including 2D structural analysis, e.g., in synthetic chemistry, metabolic studies, drug delivery), continuous flow quality control, and fast quantitative analysis (unbiased for samples with long relaxation times). Also, microfluidic NMR enables the hyphen-

Received: September 25, 2016
Accepted: January 23, 2017
Published: January 23, 2017

DOI: 10.1021/acs.analchem.6b03784
Anal. Chem. 2017, 89, 2296−2303

ation of NMR to chromatographic separation techniques.[3,27−29] The monitoring of chemical reactions has successfully been performed in a microcoil NMR setup by several groups.[13,30−33] The small volumes permits an efficient use of solvents, which is less expensive, e.g., when deuterated solvents are used, and environmentally friendly because of the low solvent consumption. When a mass-limited sample can be completely dissolved in the small microcoil detection volume, one can work with higher analyte concentrations than when using the larger conventional NMR detection volume. When using higher analyte concentration, methods, such as solvent suppression, become easier. It should be noted that if sufficient sample with a fixed concentration is available, conventional NMR gives a higher sensitivity, but for a limited amount of sample the sensitivity is better for the smallest coil matching the sample volume.[1,34]

The stripline resonator is a straight flat wire that is used to generate and detect the radio frequency (rf) fields in the NMR experiments. The stripline NMR chip is manufactured using microfabrication techniques such as photolithography, electroplating, and wet chemical etching.

The ground planes ("shields") surrounding the stripline enclose the generated rf B_1 field. The boundary conditions imposed by the ground planes arrange the field lines parallel to the stripline surface, as a result the B_1 field is homogeneous, which is crucial for complex pulse sequences. The sample volume is scaled down to 150 nL in the design used in the present study. Standard microfluidics can be connected to the stripline NMR chip, making it possible to continuously flow the sample during acquisition. Continuous-flow or recycled-flow NMR[35,36] can be advantageous, for example, for samples that have long relaxation times, mass-limited samples, or unstable samples.

The stripline design is scalable, so one can use an optimal volume for each specific application. We have previously shown the application of this setup for real-time monitoring of fast chemical reactions, acquiring steady state ^{1}H signals during the first minutes of the reaction.[37] Furthermore, the upright geometry of the stripline is particularly convenient for realizing a flow setup with straight capillaries running through the probehead.

Proton NMR spectra are very information-rich as such. However, more detailed information can be obtained from two-dimensional (2D) NMR, ^{13}C NMR, and/or heteronuclear NMR experiments. Investigating the correlations within the molecules and the surrounding of the carbon nuclei is of considerable use in molecular structure determination. Particularly for the analysis of mass-limited complex molecules or mixtures, the addition of an X-channel is a very useful feature. Here, the possibility to add flow is particularly helpful to overcome SNR issues due to long T_1 relaxation times of X-nuclei compared to ^{1}H spins. Finally, for in situ monitoring of fast reactions the higher resolution of, e.g., ^{13}C spectra can be a valuable asset. In this paper we demonstrate, as a proof of principle, some common ^{1}H 2D, ^{13}C, and heteronuclear NMR experiments during flow of the model compounds ethyl crotonate and menthol in a microfluidic stripline probe.

EXPERIMENTAL SECTION

Chemicals. Ethyl crotonate (99%) and menthol (99%) were obtained from Sigma-Aldrich and used without further purification. Chloroform-d_3 + 0.05%v/v TMS (Cambridge Isotopes Laboratories, Inc.) was used as a solvent. A 20 vol % ethyl crotonate solution in chloroform-d_3 (1.6 M) and a 30 vol % menthol solution in chloroform-d_3 (2 M) were used for the stripline NMR flow experiments. For the ^{13}C channel, pulse length and decoupling parameters were set up by using a 1 M D-glucose-1-^{13}C (CAMPRO Scientific, Veenendaal, The Netherlands) solution in D_2O.

Stripline rf-Coil. The stripline rf-coil[17,20] consists of a copper strip through which the radio frequency (rf) current runs (see the pictures in Figure 1). In the middle part of the chip, the width of the strip is constricted to 0.6 mm (for a section of 3 mm length) in order to enhance the rf field strength in this area and therefore localize detection to this area. The boundaries of the resonator are formed by flat copper shielding layers parallel to the strip, so the magnetic field lines are arranged parallel to the surface. In the region of homogeneous and high B_1 field, two microfluidic microchannels run along both sides of the strip. In the experiments described here, only one of the microchannels is used; however, the other microchannel can be used, e.g., for a reference sample or D_2O for the locking of the NMR spectrometer.

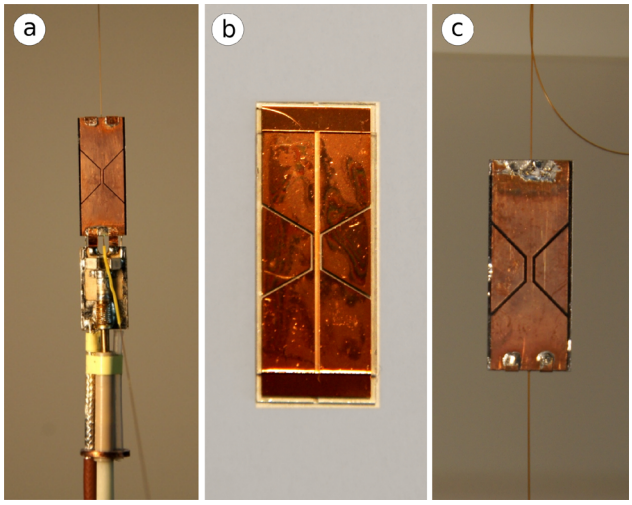

Figure 1. NMR stripline chips used in this study: chip a, chip b, and chip c.

The stripline chips a, b, and c used in the present work are displayed in Figure 1, and the design differs from the design that was described in our previous work.[20] Technical details can be found in the Supporting Information. The design of chips a and c was motivated by aiming for straightforward connection of microfluidics and a higher filling factor. The substrates are borosilicate glass into which the microchannels are etched in such a way that optimal use is made of the space between stripline and shielding. The inlet and outlet are positioned on the top and bottom of the chips and flow is enabled by fused silica (FS) capillaries glued into the chip, which ensures a convenient microfluidic connection. Chip c, which has a detection volume of approximately 215 nL, was fabricated first; however, it did not give as good sensitivity results as expected. Chip a was made from thinner substrates in order to make a smaller detection volume of 165 nL. The sensitivity improved, but unfortunately the chip turned out to be fragile, so that leakages occurred in the substrate itself as well as in the connecting capillaries. For chip b, FS substrates are used, because this material has a better dielectric performance, so that dielectric losses from the substrate that affect the sensitivity can

DOI: 10.1021/acs.analchem.6b03784
Anal. Chem. 2017, 89, 2296−2303

be avoided. Chip b was designed to be more robust, with a diced channel which contains a separate and replacable FS capillary with standard dimensions to make leak-proof and simple connection to a microfluidic setup or use of a sample plug in the capillary, so that a detection volume up to 145 nL results. The observation factor is the fraction of the sample volume from which the NMR signal is observed,[34] which is high when sample plugs are used, since up to 100% of the sample can be placed in the detection volume. However, the filling factor, defined as the part of the detection volume which is occupied by the observed part of the sample,[34] is lower in chip b as the space between stripline and shielding is not as efficiently used as in chips a and c. The spectral resolution obtained with chip b is not as good as expected, which is attributed to irregularities in the microfluidic channel resulting from the dicing procedure. Nevertheless, considering the benefits of the design of chip b, it is worthwhile to explore the possibilities of this chip, e.g., the chip is directly accessible from the outside allowing not only flow experiments, but it is also possible to use a piece of capillary as a tiny NMR tube for mass-limited samples. Since having a high resolution is not as critical in ^{13}C NMR measurements as in ^{1}H NMR measurements, in this work we demonstrate chip b for the ^{13}C experiments. Descriptions of the fabrication of chips a and c are given in ref 38 and of chip b in the Supporting Information.

The stripline chips can be placed in one of two homebuild probes; a single resonance probe with a ^{1}H channel and a double resonance probe with a ^{1}H channel and a variable frequency X-channel. In order to enable continuous flow, a syringe pump is attached to the inlet and outlet capillaries via standard microfluidic components. Information regarding the probeheads and microfluidics can be found in the Supporting Information.

Acquisition and Processing. The spectra were taken at room temperature on a VNMRS 600 MHz Varian NMR spectrometer with VNMRJ software. MatNMR[39] was used for data processing and plotting, and ACD/NMR Processor (Advanced Chemistry Development, Inc.)[40] was used for plotting of the correlation spectra.

RESULTS AND DISCUSSION

Practical Considerations. An important feature of in situ microfluidic NMR measurements is that by continuously flowing the sample through the detection volume during acquisition, the spins that have received an rf pulse are continuously replaced by spins with thermal equilibrium polarization that have not yet received an rf pulse. The apparent relaxation delays of the experiment are affected, as both the observed spin−lattice relaxation time (T_1^{obs}) and the observed spin−spin relaxation time (T_2^{obs}) decrease.[35,41,42] The stationary value of T_1 reflects the time constant for the spins to return to thermal equilibrium after receiving an rf pulse, which poses limitations on the repetition rate. However, when the analyte flows through the detection area during acquisition, the spins can be refreshed faster than the stationary value of T_1, the acquisition delay between scans can be shortened. In effect, measurement time can be decreased by using continuous flow during acquisition for samples with long T_1 relaxation times. At a moderate flow rate of 5 μL/min, the detection volume of 150 nL is refreshed in almost 2 s, whereas for the 215 nL detection volume it takes 3 s to completely replenish the detection volume. At a flow rate of 15 μL/min, this retention time decreases to 0.6 and 1 s, respectively. The repetition rate of the scans can be increased and thereby the signal-to-noise ratio per unit time. Here it is assumed that the sample flows linearly through the channel, but in reality a more complicated flow profile arises because of the laminar pressure-driven flow. The part of the sample close to the walls of the capillary has a lower flow rate because of the parabolic Poiseuille flow profile, while the center part has a higher flow rate. This might affect the accuracy of quantifiability of the experiments.

From the moment the analyte flows into the magnet until the detection scan in the stripline, polarization build-up takes place. When the flow rate increases, the time in the magnet is shortened and it is important to verify that the time for polarization build-up is long enough to reach the thermal equilibrium polarization. In order to fully polarize the spins in the sample, a build-up time of $5T_1$ is needed. In our setup the sample flows through a 250 μm i.d. capillary of approximately 60 cm long before arriving at the stripline. At the highest used flow rate of 15 μL/min, the build-up time is still 37.5 s, long enough for most spins in our samples to achieve thermal equilibrium polarization. A longer build-up time can easily be established by increasing the volume of the analyte inside the magnet before reaching the stripline, e.g., by using a longer capillary trajectory inside the magnet toward the NMR detector.

Flowing the sample out of the detection area during acquisition can result in line broadening, since the recorded free induction decay (FID) is shortened by nuclear spins flowing out of the detection area during acquisition. When the residence time of spins in the detection coil decreases, the effective decay time of the FID decreases, so that the observed relaxation time T_2^{obs} decreases as well.[42] The observed relaxation time depends on the residence time τ and the stationary value of the relaxation time T_2^{stat}: $\frac{1}{T_2^{obs}} = \frac{1}{T_2^{stat}} + \frac{1}{\tau}$. For the smallest detection volume (145 nL) and the highest flow rates (15 μL/min), an estimated increase of ∼0.4 Hz can be expected for line widths of approximately 3 Hz (full-width at half-maximum). In the present setup and for the used flow rates, this broadening effect does not significantly affect the spectra. A broadening of 1 Hz, i.e., from 3 to 4 Hz, would be expected at flow rates of approximately 30 μL/min.

One-Dimensional ^{1}H and ^{13}C Spectra. NMR measurements can be performed, while the solution is flowing at constant flow rate through the stripline microchannel. The proton spectra of ethyl crotonate and menthol during flow are shown in Figure S5 in the Supporting Information. The spectra can be assigned in agreement with the literature.[43,44] We find a resolution of 2.8 Hz for ethyl crotonate and 2.7 Hz for menthol (measured full-width half-maximum). No significant line broadening due to flow was observed for the employed flow rates.

We tested the ^{13}C channel of the HX dual channel probe with chip b. The experiments were first optimized using a 1 M ^{13}C-labeled D-glucose-1-^{13}C solution. The 90° pulse was found to be 3.5 μs using 240 W rf power. The decoupler is set to 2W WALTZ-16 proton-decoupling with NOE enhancement. To determine the sensitivity of the ^{13}C channel, a spectrum accumulating 1000 scans was acquired for this test sample, from which a signal-to-noise ratio of 0.5 for a single scan was deduced. This corresponds to a limit of detection (LOD) of approximately $1 \cdot 10^{15}$ spins/$\sqrt{\text{Hz}}$ for the ^{13}C nuclei, defined by the number of spins needed in 1 Hz bandwidth in order to obtain a signal-to-noise ratio of 1.[17]

DOI: 10.1021/acs.analchem.6b03784
Anal. Chem. 2017, 89, 2296−2303

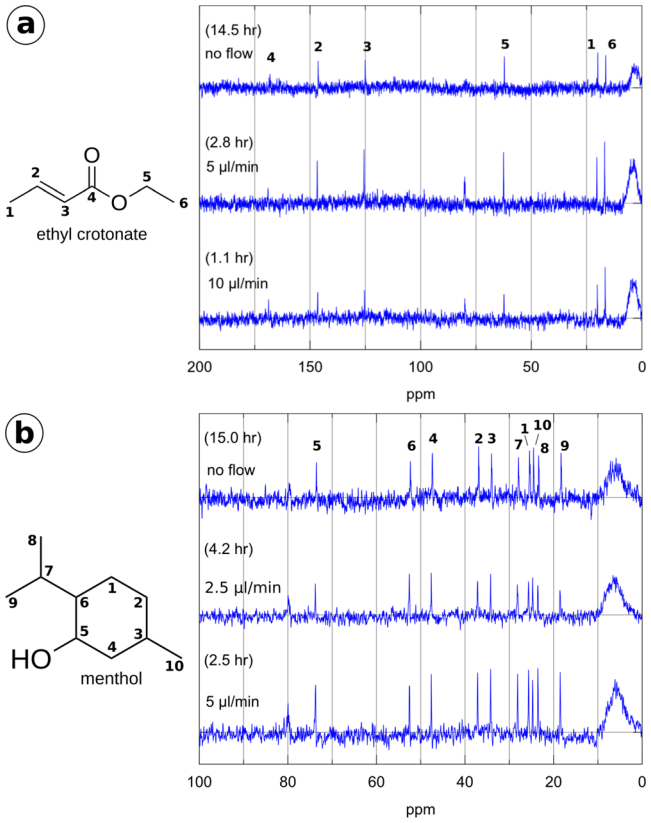

Figure 2. ^{13}C measurements using stopped flow or continuous flow in (a) ethyl crotonate (20 vol %) and (b) menthol (30%). The HX dual channel probe fitted with chip b was employed. Each spectrum was recorded by accumulating 4096 scans. For increasing flow rates, the repetition rate was increased using shorter recycle delays and acquisition times. Ethyl crotonate was measured with a recycle delay of 12 s without flow, which decreased to 1.5 and 0.5 s, for 5 μL/min and 10 μL/min flow rates, respectively. The acquisition time was 0.25 s for stopped flow and decreased to 0.1 s for the highest flow rate. Overall, this decreased the experiment time from 14.5 to 1.1 h. Menthol was measured with an acquisition delay of 12.5 s without flow and 3 and 1.8 s for 2.5 μL/min and 5 μL/min flow rates, respectively. The acquisition time was 0.25 s for the measurement without flow and 0.1 s for the two measurements in flow. Measurement time decreased from 15.0 to 2.5 h.

After finding the optimal pulse and decoupling settings, stopped flow ^{13}C measurements of ethyl crotonate (20 vol %) and menthol (30%) were successfully performed, as displayed in Figure 2. Relaxation times T_1 can be very long for ^{13}C nuclei, for protonated carbon atoms the values lie typically in the range from 0.1−10 s, whereas quaternary carbon atoms have values ranging from 10 up to 300 s.[45]

For ethyl crotonate, we found experimental T_1 relaxation times varying between 6 and 18 s (quaternary carbon 4 in Figure 2a), i.e., the relaxation delay in the stopped-flow experiments was too short to ensure quantitative interpretation of the resonances. In continuous flow NMR, the sample in the detection volume is completely refreshed faster than the relaxation time T_1, so the acquisition delay can be shortened and thus the overall measurement time significantly decreased for slow relaxing nuclei.[41] At a flow rate of 10 μL/min, the sample has been inside of the magnet for 56 s, which is equivalent to $9T_1$ for the fastest relaxing nuclei (T_1 is 6 s) and $3T_1$ for the quaternary carbons (T_1 is 18 s) of ethyl crotonate. We measured a spectrum acquiring 4096 scans in 14.5 h using a delay of 12 s between scans in the case of stopped flow and could obtain a similar spectrum in 2.8 h at 5 μL/min flow rate and in 1.1 h at 10 μL/min flow rate using a recycle delay of 1.5 and 0.5 s, respectively. During continuous flow, the line widths of the peaks increased from approximately 4 Hz in the stopped flow spectra to around 7−8 Hz under continuous flow conditions. The ^{13}C T_1 values for menthol varied from 2 to 6 s. The stationary (stopped flow) measurement of 4096 scans took 15.0 h with a delay of 12.5 s, whereas this took only 4 h at a flow rate of 2.5 μL/min and 2.5 h at a flow rate of 5 μL/min, using a delay of 1.8 s. As a measure of accuracy of the experiments, the peaks in the spectra have been integrated after peak deconvolution of the baseline corrected spectra. The standard deviations for the peaks are 8%, 9%, and 10%, respectively, for the menthol spectra acquired at flow rates of 5 μL/min, 2.5 μL/min, and stopped flow. The standard deviations for the peaks of ethyl crotonate are 36%, 10%, and 12% for the experiments using flow rates of 10 μL/min, 5 μL/min, and stopped flow.

In order to obtain quantitative results, all spins in the detection volume should be fully polarized, i.e., have been in the magnetic field for 3−5 T_1 before a pulse is applied, to fully contribute contribute to the signal. In these experiments, the repetition rate is somewhat higher than the time for completely refreshing the detection volume. Furthermore, the laminar Poiseuille flow profile causes a variation in the velocity of the flow that may cause a small decrease in the intensity for nuclei with a T_1 larger than the recycle delay. However, this is only observed for peak 4 of ethyl crotonate, the T_1 value of this quaternary carbon is 18 s, which is much larger than the repetition rate. The other carbon atoms of ethyl crotonate have T_1 values of around 6−7 s, and no effect of decreasing intensity with changing flow rate is found. The T_1 values of menthol are around 6 s for three of the nuclei and around 3 s for the rest. In the stopped flow experiment, the peaks of carbon atoms with a shorter T_1 have a higher intensity (averaged 105%) than the peaks of carbon atoms with a longer T_1 (averaged 90%). For the measurements in continuous flow, this difference is not present.

The average value of the SNR (defined by the peak height divided by the rms (root-mean-square) of the noise over a 200 Hz bandwidth) of all peaks in the spectrum except quaternary carbon peak 4 is 10.6 for the stopped flow experiment and increases to 15.2 and 13.5 for the spectra measured in 5 and 10 μL/min flow rates, respectively. The lowest intensity peaks have an SNR of 8.5, 12.1, and 10.0 for the stopped flow, 5, and 10 μL/min flow measurements, meaning that if we aimed for an SNR of at least 10 the spectra could have been obtained in 20 h, 2 h, or 1 h under the given flow conditions.

For menthol, the average SNR measured in stopped flow was 9.3, which increased under continuous flow conditions to 13.1 and 16.0 for 2.5 and 5 μL/min flow, respectively. The lowest measured SNR was 8.0, 10.5, and 13.5 for stopped flow, 2.5, and 5 μL/min flow, so that a spectrum with a minimum SNR of 10 could have been measured in 23.5 h, 3.5 h, and 1.4 h, respectively.

Applying continuous flow during the acquisition consumed 750 μL for experiments using 2.5 μL/min and 5 μL/min flow rate and 600 μL for the experiments using 10 μL/min flow rate. Clearly a setup flowing in fresh sample continuously, as in the current setup, is not feasible for mass-limited samples. In that case, flow NMR is still feasible but with a small storage volume close to the stripline. The size of the storage volume for optimal

DOI: 10.1021/acs.analchem.6b03784
Anal. Chem. 2017, 89, 2296−2303

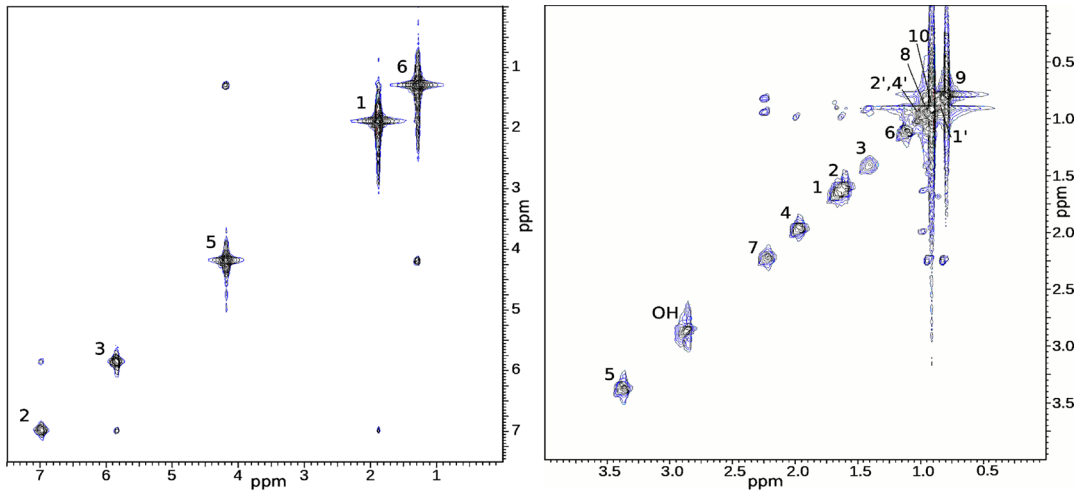

(a) Ethyl crotonate, 15 μl/min (b) Menthol, 1 μl/min

Figure 3. Continuous flow COSY measurements at (a) 15 μL/min flow rate for ethyl crotonate (20 vol %) and (b) at 1 μL/min flow rate for menthol (30%), performed in the ^{1}H probe fitted with chip a. Both spectra were taken accumulating 4 scans for 256 t_1-increments. A relaxation delay of 1 s was taken into account for ethyl crotonate (20 vol %) using 15 μL/min flow and 2 s for menthol (30%) at a flow rate of 1 μL/min. The experiment time was 30 min for ethyl crotonate and 47 min for menthol. Zero filling up to 8192 × 4096 points and a line broadening of 3 Hz for the direct dimension and 5 Hz for the indirect dimension was applied for ethyl crotonate and 1 Hz broadening and a sine-function for menthol.

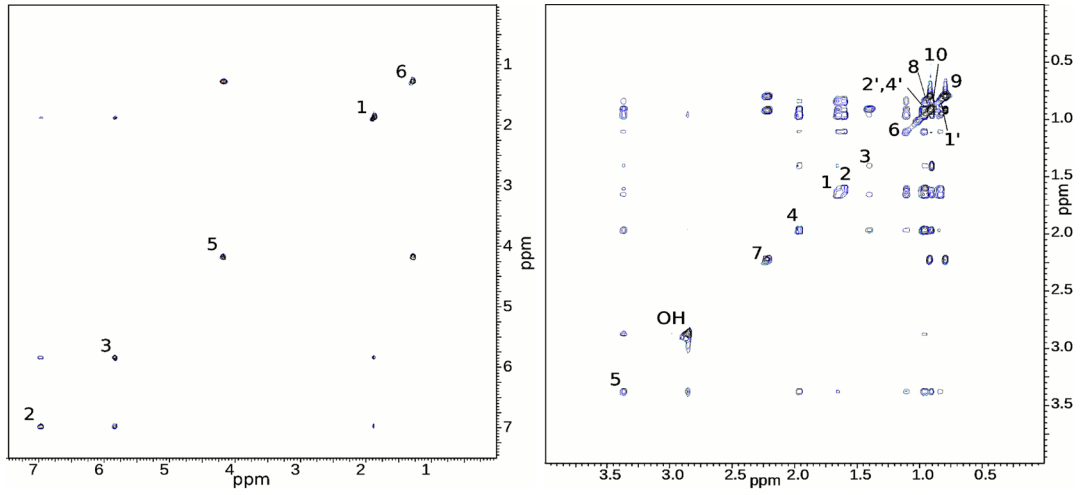

(a) Ethyl crotonate, 1 μl/minute (b) Menthol, 15 μl/minute

Figure 4. Continuous flow TOCSY measurements, at a flow rate of (a) 1 μL/min for ethyl crotonate and (b) 15 μL/min for menthol, performed in the ^{1}H probe fitted with chip a. (a) 4 scans for 512 t_1-increments were acquired for ethyl crotonate (20 vol %) and (b) 4 scans and 256 increments for menthol (30%). For ethyl crotonate, an acquisition delay of 3 s was taken into account. The experiment time was 4 h and 20 min. For menthol the acquisition delay was 1 s and the experiment time was 1 h and 30 min. For both experiments, a mixing time of 50 ms, using an MLEV17 spinlock and a trim pulse of 2 ms was used. Zero-filling up to 8192 × 2048 and a line broadening of 1 Hz was applied in both directions.

SNR is then a trade-off between sample availability and length of T_1^{stat}.

We did not further increase the flow rate to speed up the measurement because it was experimentally observed that a delay between scans is needed to take into account the decoupling period before acquisition and the duty cycle of the decoupler to prevent heating of the detection area of the chip.

Finally, it has to be noted that the resolution obtained with chip b is suboptimal, probably because of susceptibility broadening, which is attributed to imperfections in the microchannel as a result from the dicing procedure disturbing the B_0 homogeneity. It is expected that a modification to the stripline NMR chip fabrication process which avoids the dicing procedure will result in a more homogeneous B_0 field, so that a higher spectral resolution can be achieved. This will further enhance the effective signal-to-noise ratio of the spectra, so that the experimental time to achieve the same SNR at a given resolution can be further decreased.

Two Dimensional Correlation Spectroscopy. For structural elucidation, two-dimensional NMR is a valuable addition to the one-dimensional NMR experiments. Common experiments are correlation spectroscopy (COSY[46]) and total correlation spectroscopy (TOCSY[47]). Both experiments show correlations of proton spins within the molecule. A COSY spectrum shows cross peaks for directly coupled spins over one or more bonds, whereas a TOCSY spectrum also can be used for studying longer range couplings depending on the mixing time.

COSY and TOCSY spectra have been acquired both at low and high flow rates as shown in Figures 3 and 4. Considering

DOI: 10.1021/acs.analchem.6b03784
Anal. Chem. 2017, 89, 2296−2303

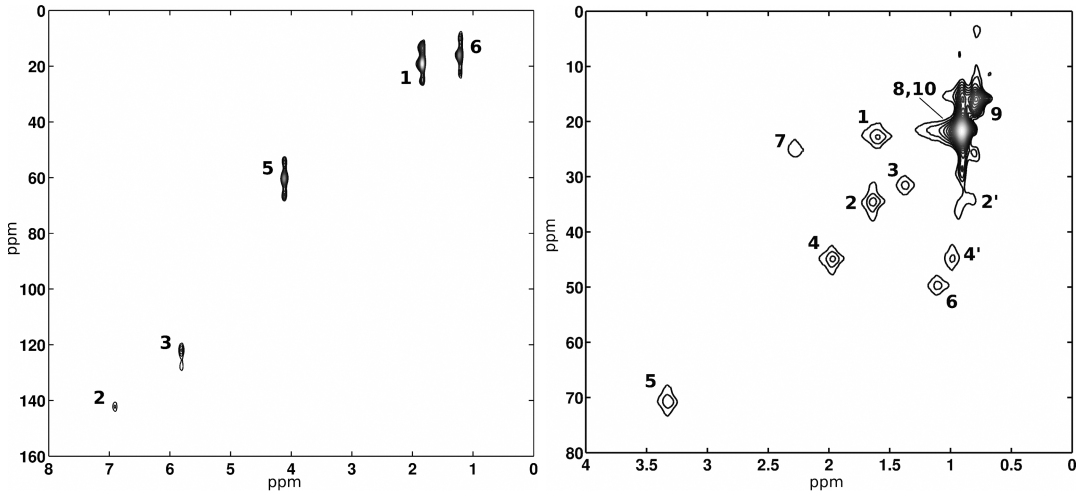

(a) Ethyl crotonate, 7 μl/min (b) Menthol, 0.5 μl/min

Figure 5. HMQC spectra of (a) ethyl crotonate (20 vol %) and (b) menthol (30%) with flow rates of 7 μL/min for ethyl crotonate and 0.5 μL/min for menthol, performed in the HX channel probe and chip c. We acquired 400 scans for 64 increments for ethyl crotonate and 512 scans with 128 increments for menthol. The acquisition delays were 1 and 1.2 s, respectively, and a BIRD delay of 0.6 and 0.5 s. The pulse sequence delays were adjusted to a one-bond $^{1}H-^{13}C$ coupling constant of 145 Hz.

the small molecules, we used short mixing times (50 ms) with an MLEV17[48] spinlock for the TOCSY. The line widths are around 5 Hz in the F2 dimension and 10 Hz in the F1 dimension for the TOCSY spectra. For the COSY spectra, however, the cross peaks are around 30 Hz in the F1 dimension. In COSY experiments, the cross peaks have an antiphase absorption line shape, while the diagonal peaks have a broad, dispersion lineshapes. For larger line widths, the wide tail of the diagonal peak may obscure the cross peaks and the intensity of the cross peaks may be diminished due to the antiphase lineshapes. Cancelation of the cross peaks can arise from these lineshapes and is a known disadvantage of COSY experiments.[43] TOCSY experiments do not suffer from these cancelation effects for broad lines and are therefore more preferred. So it is interesting to perform TOCSY experiments in the stripline chip, especially in the case of unstable samples or reaction monitoring in continuous flow, if the sample is not stable during the acquisition time of two-dimensional NMR experiments in conventional NMR. Alternatively, mass-limited samples can be measured in a static plug in a FS capillary in chip b, as described before.

Finally, double-resonance experiments can be performed in the dual-channel probe providing relevant structural information. Heteronuclear multiple-quantum correlation spectroscopy (HMQC)[49] correlates proton and carbon spins that are directly coupled. After establishing the optimal decoupling and pulse length parameters on D-glucose-1-^{13}C, HMQC experiments were performed for both model compounds using low (0.5 μL/min) and medium (7 μL/min) flow rates (Figure 5). The experimental time for the measurement of ethyl crotonate at a 7 μL/min flow rate was 25 h with a consumption of 10 mL solution. The menthol spectrum was obtained in 69 h, consuming 2 mL of solution (at 0.5 μL/min).

Comparison of the Chips. Good resolution and sensitivity are crucial in obtaining informative NMR spectra. Since the copper stripline structure is defined with the same geometry (i.e., a 3 mm long constriction) in each of the chips employed in this study, the results can be directly compared to give information about their performance.

The sensitivity of the stripline NMR chip has a substantial effect on the efficiency of the measurement, i.e., the signal-to-noise ratio in the spectrum obtained per unit time. A good measure of sensitivity is the limit of detection (LOD), defined as the number of spins needed in 1 Hz bandwidth in order to obtain a signal-to-noise ratio of 1.[17] The LOD for protons (LOD_H) is measured from a single-scan ethanol free-induction-decay (FID). For proton detection in chips a and b, we found a similar LOD_H of $2.5-4 \times 10^{13}$ spins/$\sqrt{\text{Hz}}$, respectively, whereas for chip c, a LOD_H of 2×10^{14} spins/$\sqrt{\text{Hz}}$ was found. The significantly lower detection limit (LOD_H) of chips a and b indicates a higher sensitivity of these chips compared to the sensitivity of chip c. The theoretically expected LOD_H is around 2×10^{13} spins/$\sqrt{\text{Hz}}$ for all chips but does not take into account dielectric losses due to the substrate (which can be rather large due to inclusion of, e.g., metal-oxide impurities); therefore, the low sensitivity of chip c is attributed to the nonoptimal substrate.[38]

In terms of resolution, chip a in Figure 1 was found to perform best with a line width of less than 3 Hz for the ^{1}H spectra. In the single-scan spectra of ethyl crotonate and menthol, we find for ethyl crotonate the following line widths (full-width half-maximum): chip a 2.7 Hz, chip b 7 Hz, chip c 9 Hz (estimated via deconvolution of the multiplets). Similar results were estimated from the menthol spectra, where due to overlapping peaks could not be as precisely defined. Another comparison of the spectral resolution can be made from a single-scan spectrum of ethanol (70%), having the advantage that since the concentration is high a large signal is obtained; therefore, the shimming procedure is uncomplicated. For single-scan ethanol (70%) spectra, the best resolution of chip a is approximately 2 Hz, for chips b and c the line width is around 3 Hz. The peak shape of chip b, however, contains a broad foot structure and other irregularities.

The signal-to-noise ratio (SNR) in the spectrum obviously depends on the amount of sample (concentration per unit volume vs total volume) but is also affected by the LOD and resolution provided by each chip. For ethyl crotonate, the SNR is calculated from the single scan ^{1}H spectrum using the methyl

DOI: 10.1021/acs.analchem.6b03784
Anal. Chem. 2017, 89, 2296−2303

group 6 in Figure S5a, resulting in 1080 for chip a, 168 for chip b, and 446 for chip c. For menthol, we find for chip a 3308, for chip b 238, and chip c 313 calculated using the resonances of the methyl groups 8 and 10 in Figure S5b. In conclusion, the SNR for chip a is significantly better than the SNR for chips b and c. Furthermore, we find that although the detection limit (LOD_H) of chip b is only slightly higher than for chip a, in the spectrum a relatively low SNR is found. The lower SNR in the spectrum is attributed to the loss of signal in the broad foot of the peaks and the relatively low spectral resolution, which decreases the intensity of the signal in the spectrum.

Overall, chip a gives the best results, combining a high resolution with high sensitivity. Currently, work is in progress to improve the performance of chip b, as according to theoretical calculations it should be possible to increase the signal-to-noise ratio in the spectrum by an order of magnitude. The design of chip b would enable easier measurement of small volume samples, since a sample plug can be positioned offline in the exchangeable FS capillary.

Approach for Mass-Limited Samples. For mass-limited samples, it is necessary to decrease the total sample volume that is used; therefore, we currently investigate the use of a recycled-flow[50] system using a micropump. For example, a HMQC experiment on menthol accumulating 512 scans and 128 t_1 increments, such as shown in Figure 5b, could be performed in recycled-flow at a flow rate of 15 μL/min, taking into account a T_1 of 30 s. When the time between measurement on the same part of the sample is set to T_1, the loop would need to contain approximately 7.5 μL, which corresponds to an amount of 15 μmol of menthol in our experiment. Decreasing the flow rate can further reduce the required sample volume, but the acquisition delay between scans has to be longer to account for T_1, which implies that the total experiment takes longer. In turn, a smaller acquisition delay would decrease the amount of sample that is necessary, since measurement of the same sample can be repeated faster.

Alternatively, for very small amounts of sample, it can be advantageous to concentrate all of the sample in a single plug, i.e., a droplet of concentrated sample covering the detection area embedded in a nonmixable buffer solution. This can easily be accomplished using chip b (Figure 1). Since the single-scan signal-to-noise ratio increases by concentrating the sample, measurement time can be reduced. Depending on the limitations in amount and solubility of the sample, measurement time, and T_1, one can optimize the setup using a recycled flow sample loop with a micropump or concentrating the sample in a single plug.

CONCLUSIONS

In the work presented here, we successfully performed the most common experiments that are used to elucidate structures of small organic molecules, ^{1}H NMR and ^{13}C NMR as well as homonuclear and heteronuclear correlation spectroscopy, in the stripline microfluidic NMR probe under continuous flow conditions.

Acquiring spectra in continuous flow made it possible to perform ^{13}C NMR experiments on two test compounds, ethyl crotonate and menthol, in a drastically decreased measurement time. The two-dimensional correlation spectra showed all expected peaks with no observed differences between low and high flow rates (1 and 15 μL/min, respectively). COSY and TOCSY spectra were successfully acquired for both compounds. The HMQC spectra that were obtained in continuous flow accurately showed the expected proton−carbon correlations.

The concentrations of stock solutions that were used are high (1.6 and 2.0 M), but still the plug the size of the 150 nL detection volume contains only 0.3 μmol of compound. This amount of compound, when dissolved in a 500 μL of solution, corresponds to a 0.5 mM solution in a conventional NMR tube. Considering the good signal-to-noise ratios of the proton spectra, lower concentrated samples can easily be measured on the proton channel of our setup.

Possible ways to further shorten the experiment time and/or sample volume are increasing the sample concentration and using the sample very efficiently in a sample plug or a recycled-flow system. The design of chip b as displayed in Figure 1 features a removable FS capillary, in which the sample can be positioned by hand as an alternative to continuous flow conditions. This design would therefore be perfectly suited for the measurement of concentrated sample plugs or for measuring a very small sample without the need for dilution. Moreover, a microflow system could be attached to the sample capillary straightforwardly. However, more work is needed to optimize the resolution of this chip design.

In conclusion, the results show that various stripline setups are suitable for experiments on mass-limited samples as well as for fast chemical reactions or otherwise unstable samples and can be advantageously performed in situ during flow. Attractive applications for continuous flow stripline NMR include monitoring of reaction kinetics, quality control, and fast quantitative analysis. Measuring in continuous flow can also be beneficial for obtaining ^{13}C spectra of samples with very long ^{13}C relaxation times, since in that case the detection volume can be refreshed much faster than the relaxation time.

ASSOCIATED CONTENT

Supporting Information

The Supporting Information is available free of charge on the ACS Publications website at DOI: 10.1021/acs.analchem.6b03784.

Technical details of the stripline NMR chips; fabrication details of fused silica stripline NMR chips; technical details of homebuild probes and microfluidics; and ^{1}H NMR spectra measured in continuous flow of ethyl crotonate (20 vol %) and menthol (30%) (PDF)

AUTHOR INFORMATION

Corresponding Author

*E-mail: a.kentgens@nmr.ru.nl.

ORCID

Arno P. M. Kentgens: 0000-0001-5893-4488

Present Address

§J.B.: AkzoNobel NV, Shared Research, Strategic Research Group, Zutphenseweg 10, 7418 AJ Deventer, The Netherlands.

Notes

The authors declare no competing financial interest.

ACKNOWLEDGMENTS

This research was financially supported by the ACTS-Process on a Chip Programme of The Netherlands Organization for Scientific Research (NWO). NWO is furthermore acknowledged for their support of the solid-state NMR facility for

DOI: 10.1021/acs.analchem.6b03784
Anal. Chem. 2017, 89, 2296−2303

advanced materials science. Ruud Aspers is acknowledged for acquiring the T_1 relaxation time data.

REFERENCES

(1) Webb, A. *Prog. Nucl. Magn. Reson. Spectrosc.* **1997**, *31*, 1.
(2) Hoult, D.; Richards, R. *J. Magn. Reson.* **1976**, *24*, 71.
(3) Wu, N.; Peck, T. L.; Webb, A. G.; Magin, R. L.; Sweedler, J. V. *J. Am. Chem. Soc.* **1994**, *116*, 7929.
(4) Olson, D. L.; Peck, T. L.; Webb, A. G.; Magin, R. L.; Sweedler, J. V. *Science* **1995**, *270*, 1967.
(5) Peck, T.; Magin, R.; Kruse, J.; Feng, M. *IEEE Trans. Biomed. Eng.* **1994**, *41*, 706.
(6) Kentgens, A. P. M.; Bart, J.; van Bentum, P. J. M.; Brinkmann, A.; van Eck, E. R. H.; Gardeniers, J. G. E.; Janssen, J. W. G.; Knijn, P.; Vasa, S.; Verkuijlen, M. H. W. *J. Chem. Phys.* **2008**, *128*, 052202.
(7) Fratila, R. M.; Velders, A. H. *Annu. Rev. Anal. Chem.* **2011**, *4*, 227.
(8) Badilita, V.; Meier, R. C.; Spengler, N.; Wallrabe, U.; Utz, M.; Korvink, J. G. *Soft Matter* **2012**, *8*, 10583.
(9) Jones, C. J.; Larive, C. K. *Anal. Bioanal. Chem.* **2012**, *402*, 61.
(10) Zalesskiy, S. S.; Danieli, E.; Blümich, B.; Ananikov, V. P. *Chem. Rev.* **2014**, *114*, 5641.
(11) Sun, N.; Liu, Y.; Qin, L.; Lee, H.; Weissleder, R.; Ham, D. *Solid-State Electron.* **2013**, *84*, 13.
(12) Meier, R. C.; Höfflin, J.; Badilita, V.; Wallrabe, U.; Korvink, J. G. *J. Micromech. Microeng.* **2014**, *24*, 045021.
(13) Brächer, A.; Hoch, S.; Albert, K.; Kost, H. J.; Werner, B.; von Harbou, E.; Hasse, H. *J. Magn. Reson.* **2014**, *242*, 155.
(14) Ryan, H.; Song, S.-H.; Zaß, A.; Korvink, J.; Utz, M. *Anal. Chem.* **2012**, *84*, 3696.
(15) Fratila, R. M.; Gomez, V.; Sýkora, S.; Velders, A. H. *Nat. Commun.* **2014**, *5*, 3025.
(16) Spengler, N.; Höfflin, J.; Moazenzadeh, A.; Mager, D.; MacKinnon, N.; Badilita, V.; Wallrabe, U.; Korvink, J. G. *PLoS One* **2016**, *11*, e0146384.
(17) van Bentum, P. J. M.; Janssen, J. W. G.; Kentgens, A. P. M.; Bart, J.; Gardeniers, J. G. E. *J. Magn. Reson.* **2007**, *189*, 104.
(18) Maguire, Y.; Chuang, I. L.; Zhang, S.; Gershenfeld, N. *Proc. Natl. Acad. Sci. U. S. A.* **2007**, *104*, 9198.
(19) Krojanski, H. G.; Lambert, J.; Gerikalan, Y.; Suter, D.; Hergenroder, R. *Anal. Chem.* **2008**, *80*, 8668.
(20) Bart, J.; Janssen, J. W. G.; van Bentum, P. J. M.; Kentgens, A. P. M.; Gardeniers, J. G. E. *J. Magn. Reson.* **2009**, *201*, 175.
(21) Tayler, M. C. D.; van Meerten, S. G. J.; Kentgens, A. P. M.; van Bentum, P. J. M. *Analyst* **2015**, *140*, 6217.
(22) Finch, G.; Yilmaz, A.; Utz, M. *J. Magn. Reson.* **2016**, *262*, 73.
(23) Sans, V.; Cronin, L. *Chem. Soc. Rev.* **2016**, *45*, 2032.
(24) Moule, A. J.; Spence, M. M.; Han, S. I.; Seeley, J. A.; Pierce, K. L.; Saxena, S.; Pines, A. *Proc. Natl. Acad. Sci. U. S. A.* **2003**, *100*, 9122.
(25) Granwehr, J.; Harel, E.; Han, S.; Garcia, S.; Pines, A.; Sen, P. N.; Song, Y. Q. *Phys. Rev. Lett.* **2005**, *95*, 075503.
(26) McDonnell, E. E.; Han, S.; Hilty, C.; Pierce, K. L.; Pines, A. *Anal. Chem.* **2005**, *77*, 8109.
(27) Laude, D. A., Jr.; Wilkins, C. L. *Anal. Chem.* **1984**, *56*, 2471.
(28) Albert, K. *J. Chromatogr. A* **1995**, *703*, 123.
(29) Lindon, J. C.; Nicholson, J. K.; Wilson, I. D. *Prog. Nucl. Magn. Reson. Spectrosc.* **1996**, *29*, 1.
(30) Ciobanu, L.; Jayawickrama, D. A.; Zhang, X.; Webb, A. G.; Sweedler, J. V. *Angew. Chem., Int. Ed.* **2003**, *42*, 4669.
(31) Kakuta, M.; Jayawickrama, D. A.; Wolters, A. M.; Manz, A.; Sweedler, J. V. *Anal. Chem.* **2003**, *75*, 956.
(32) Wensink, H.; Benito-Lopez, F.; Hermes, D. C.; Verboom, W.; Gardeniers, J. G. E.; Reinhoudt, D. N.; van den Berg, A. *Lab Chip* **2005**, *5*, 280.
(33) Gomez, M. V.; Rodriguez, A. M.; de la Hoz, A.; Jimenez-Marquez, F.; Fratila, R. M.; Barneveld, P. A.; Velders, A. H. *Anal. Chem.* **2015**, *87*, 10547.
(34) Olson, D. L.; Norcross, J. A.; O'Neil-Johnson, M.; Molitor, P. F.; Detlefsen, D. J.; Wilson, A. G.; Peck, T. L. *Anal. Chem.* **2004**, *76*, 2966.
(35) Sudmeier, J. L.; Günther, U. L.; Albert, K.; Bachovchin, W. W. *J. Magn. Reson., Ser. A* **1996**, *118*, 145.
(36) Laude, D. A., Jr.; Wilkins, C. L. *Macromolecules* **1986**, *19*, 2295.
(37) Bart, J.; Kolkman, A. J.; Oosthoek-de Vries, A. J.; Koch, K.; Nieuwland, P. J.; Janssen, J. W. G.; van Bentum, P. J. M.; Ampt, K. A. M.; Rutjes, F. P. J. T.; Wijmenga, S. S.; Gardeniers, J. G. E.; Kentgens, A. P. M. *J. Am. Chem. Soc.* **2009**, *131*, 5014.
(38) Bart, J. *Stripline-based microfluidic devices for high-resolution NMR spectroscopy*. Ph.D. Thesis, University of Twente, Enschede, The Netherlands, 2009.
(39) van Beek, J. D. *J. Magn. Reson.* **2007**, *187*, 19.
(40) *ACD/NMR Processor*, Academic Edition; 2010.
(41) Laude, D. A., Jr.; Lee, R. W. K.; Wilkins, C. L. *J. Magn. Reson.* **1984**, *60*, 453.
(42) Fyfe, C.; Cocivera, M.; Damji, S.; Hostetter, T.; Sproat, D.; O'Brien, J. *J. Magn. Reson.* **1976**, *23*, 377.
(43) Claridge, T. D. W. *High-Resolution NMR Techniques in Organic Chemistry*; Tetrahedron Organic Chemistry, Vol. *27*; Elsevier: Amsterdam, The Netherlands, 2009.
(44) Braun, S.; Kalinowski, H.-O.; Berger, S. *100 and More Basic NMR Experiments: A Practical Course*; Wiley VCH: Weinheim, Germany, 1996.
(45) Abraham, R.; Fischer, J.; Loftus, P. *Introduction to NMR Spectroscopy*; Wiley: Chichester, U.K., 1988.
(46) Aue, W. P.; Karhan, J.; Ernst, R. R. *J. Chem. Phys.* **1976**, *64*, 4226.
(47) Bax, A.; Davis, D. *J. Magn. Reson.* **1985**, *65*, 355.
(48) Levitt, M.; Freeman, R.; Frenkiel, T. *J. Magn. Reson.* **1982**, *47*, 328.
(49) Bax, A.; Subramanian, S. *J. Magn. Reson.* **1986**, *67*, 565.
(50) Ha, S. T. K.; Lee, R. W. K.; Wilkins, C. L. *J. Magn. Reson.* **1987**, *73*, 467.

DOI: 10.1021/acs.analchem.6b03784
Anal. Chem. 2017, 89, 2296−2303